1056 *Biochemistry* **2010,** *49,* 1056–1058
DOI: 10.1021/bi902079y

BIOCHEMISTRY
including biophysical chemistry & molecular biology
Rapid Report

Crystal Structure of the Catalytic Domain of Human PARP2 in Complex with PARP Inhibitor ABT-888[†]

Tobias Karlberg, Martin Hammarström, Patrick Schütz, Linda Svensson, and Herwig Schüler*

Structural Genomics Consortium, Department of Medical Biochemistry and Biophysics, Karolinska Institutet, Scheeles väg 2, 17177 Stockholm, Sweden

Received December 4, 2009; Revised Manuscript Received January 15, 2010

ABSTRACT: Poly-ADP-ribose polymerases (PARPs) catalyze transfer of ADP-ribose from NAD^+ to specific residues in their substrate proteins or to growing ADP-ribose chains. PARP activity is involved in processes such as chromatin remodeling, transcription control, and DNA repair. Inhibitors of PARP activity may be useful in cancer therapy. PARP2 is the family member that is most similar to PARP1, and the two can act together as heterodimers. We used X-ray crystallography to determine two structures of the catalytic domain of human PARP2: the complexes with PARP inhibitors 3-aminobenzamide and ABT-888. These results contribute to our understanding of structural features and compound properties that can be employed to develop selective inhibitors of human ADP-ribosyltransferases.

Poly-ADP-ribose polymerases (PARPs) are ADP-ribosyltransferases; they cleave NAD^+ into ADP-ribose and nicotinamide and transfer the ADP-ribose units onto their substrates (*1*, *2*). Family members PARP1, PARP2, and PARP3 and the tankyrases catalyze ADP-ribosyl transfer and poly-ADP-ribose chain elongation. PARP1, which is responsible for the majority of ADP-ribosyltransferase activity in human cells, exerts at least some of its physiological functions as a heterodimer with either PARP2 (*3*−*5*) or PARP3 (*6*). PARP1 and PARP2 bind to stalled replication forks induced by DNA damage and recruit damage repair machinery to sites of DNA damage and are activated for DNA base excision repair (*3*, *7*). Thus, inhibition of PARP activity can affect DNA repair; this is a promising strategy for cancer therapy, in particular in homologous recombination deficient cancers that rely upon this pathway (*8*).

The 17 human PARP proteins share only between 18 and 45% pairwise sequence homology in their catalytic domains, but crystal structures indicate their structure is conserved and the mode of NAD^+ cofactor binding is rather similar. The canonical PARPs share a H-Y-E sequence motif in their active sites, as well as a tyrosine side chain that, in analogy with mono-ADP-ribosyltransferases, presumably stacks with the nicotinamide moiety of the NAD^+ cosubstrate (*9*). A number of small molecule PARP inhibitors that mimic NAD^+ have been developed; several (*10*−*12*), among them ABT-888, also known as A-861695 (*13*), are presently in clinical trials. High-resolution crystal structures of such inhibitors bound to PARP catalytic sites are essential for an in-depth understanding of the binding mode of these compounds, evaluation of the risks and mechanisms of their potential side effects, and optimization of compound selectivity and specificity.

Here, we present the structure of the catalytic domain of human PARP2 in complex with the nicotinamide mimic, 3-aminobenzamide (3-AB), and with the potent PARP1 and PARP2 inhibitor, ABT-888 (Table 1). The protein shares extensive structural similarity with PARP1 (*14*), PARP3 (*15*), and the mouse ortholog (*16*) (Figure 1A). Our two PARP2 structures show virtually identical arrangements of secondary structural elements. PARP2 structure 3kjd superimposes to a root-mean-square deviation (rmsd) of 0.8 Å with mouse PARP2 (1gs0, 315 Cα atoms), 1.4 Å with human PARP1 (2rd6, 313 Cα atoms), and 1.9 Å with human PARP3 (3c4h, 300 Cα atoms).

All publicly available structures of PARP inhibitor complexes show compound anchoring in the pocket that retains the nicotinamide moiety after NAD^+ cleavage. One of the simplest such compounds is 3-AB; it resembles nicotinamide and has been cocrystallized with several PARP proteins. Extension of the compounds into the donor site and toward the acceptor loops can then be used to improve affinity and isoform selectivity (*17*). The success of this concept is illustrated in the structure of ABT-888 (*18*).

Our crystal structures show, not surprisingly, that ABT-888 and 3-AB are anchored in the nicotinamide pocket in a very similar manner (Figure 1B). The Tyr473 side chain stacks with the imidazole ring, and the carboxamidyl forms hydrogen bonds with the Ser470 hydroxyl and with the Gly429 backbone. In addition, the Glu558 carboxyl makes a water-mediated interaction with the N-3 atom of the benzimidazole of ABT-888 and with the 3′-substituted amide of 3-AB (Figure 1B,C).

The crystal structure of the ABT-888 complex suggests interactions that may explain the high affinity of PARP2 for the inhibitor (*18*). The Tyr462 side chain interacts with the cyclic amine (pyrroline) substituent of the benzamidine ring, and the N-2 atom of the pyrrolidine forms a water-mediated bridge to the Gly429 backbone (Figure 1C). Notably, the pyrrolidine N-2 atom also connects the inhibitor to a structural element outside the catalytic site. It forms a water-mediated linkage to the Glu335 carboxyl in α-helix 5 of the N-terminal helix bundle domain that is present only in PARP1−PARP3 and vPARP/PARP4. The methyl substituent of the cyclic amide, which was shown to significantly increase the potency of this compound and similar compounds (*18*), does not interact with any hydrophobic protein

[†]This work was supported by Wellcome Trust, GlaxoSmithKline, Genome Canada, the Canadian Institutes of Health Research, the Ontario Innovation Trust, the Ontario Research Development Challenge Fund, the Canadian Foundation for Innovation, VINNOVA, The Knut and Alice Wallenberg Foundation, The Swedish Foundation for Strategic Research, the Karolinska Institutet, the Swedish Cancer Society, the Swedish Research Council, and the Swedish Cancer Foundation.

*To whom correspondence should be addressed. Phone: ++46-8-524-86843. Fax: ++46-8-524-86868. E-mail: herwig.schuler@ki.se.

 Published on Web 01/21/2010

Table 1: Crystal Parameters, Data Collection, and Refinement Statistics for PARP2−3AB (3kcz) and PARP2−ABT-888 (3kjd) Structures

Data Collection and Phasing		
PDB entry	3kcz	3kjd
space group	$P2_1$	$P2_1$
unit cell parameters	a = 58.28 Å, b = 134.72 Å, c = 58.25 Å, α = 90°, β = 117.67°, γ = 90°	a = 58.13 Å, b = 134.61 Å, c = 58.31 Å, α = 90°, β = 117.68°, γ = 90°
synchrotron beamline	DIAMOND I04	
wavelength (Å)	0.9789	
resolution range (Å)	41.0−2.0	41.0−1.95
no. of unique reflections	53327	57455
R_{merge}[a] (%)	11.2 (54.8)[b]	9.6 (56.8)[b]
completeness (%)	99.1 (99.4)[b]	99.3 (99.7)[b]
redundancy	3.1 (3.1)[b]	3.8 (3.8)[b]
$\langle I\rangle/\langle\sigma I\rangle$	10.1 (2.9)[b]	11.5 (2.7)[b]
Refinement		
resolution (Å)	41.0−2.00	41.0−1.95
R_{all}[c] (%)	18.99	18.16
R_{free}[c] (%)	23.67	23.19
rmsd for bond lengths (Å)	0.014	0.016
rmsd for bond angles (deg)	1.36	1.49
average B factor (Å^2)		
protein	19.5	22.8
ligand	11.6	16.0
solvent	23.5	29.0
Ramachandran plot[d] (%)		
most favored	98.4	97.4
allowed	100	99.8

[a] $R_{merge} = \sum_i|I_i - \langle I\rangle|/\sum\langle I\rangle$, where I is the intensity measurement for a given reflection and $\langle I\rangle$ is the average intensity for multiple measurements of this reflection. [b] Values in parentheses are for the outermost resolution shell. [c] R_{all} is defined as $\sum||F_{obs}| - |F_{calc}||/\sum|F_{obs}|$, where R_{free} is calculated for a randomly chosen 5% of reflections, which were not used for structure refinement, and R_{all} is calculated for all reflections. [d] The Ramachandran plot was calculated with Molprobity (*20*).

side chain. We believe that the methyl group creates an unpolar environment that significantly strengthens the polar interactions in the cleft, in particular the π-stacking interaction with Tyr473 and the water-mediated bond with Glu558.

In the initial characterization of ABT-888, a 2-fold selectivity for PARP2 over PARP1 was reported [K_d values of 2.9 and 5.2 nM, respectively (*19*)]. Our crystal structure suggests a mechanism for a weak bias toward PARP2. α-Helix 5 (in the N-terminal helical bundle) that contains Glu335 is closer to the active site than in both PARP1 and PARP3 (Figure 1A); these differences in interdomain angles are supported by the mouse PARP2 structure and by all published PARP1 structures, indicating they are intrinsic to these proteins rather than a crystal packing artifact. Moreover, the position corresponding to PARP2 Glu335 is occupied by the shorter aspartate (Asp766) in PARP1 (Figure 1C). The crystal structure of human PARP1 in complex with ABT-888 has been deposited in the Protein Data Bank (2rd6). However, as no structure factors were deposited, the quality of the model and of the ligand fitting cannot be evaluated. Nevertheless, the atomic coordinates suggest that the interaction between ABT-888 and the helical bundle is weak or absent in PARP1. Future studies should address other members of the PARP family and exploit the potential of structure-based approaches to achieve their selective inhibition by compounds related to ABT-888.

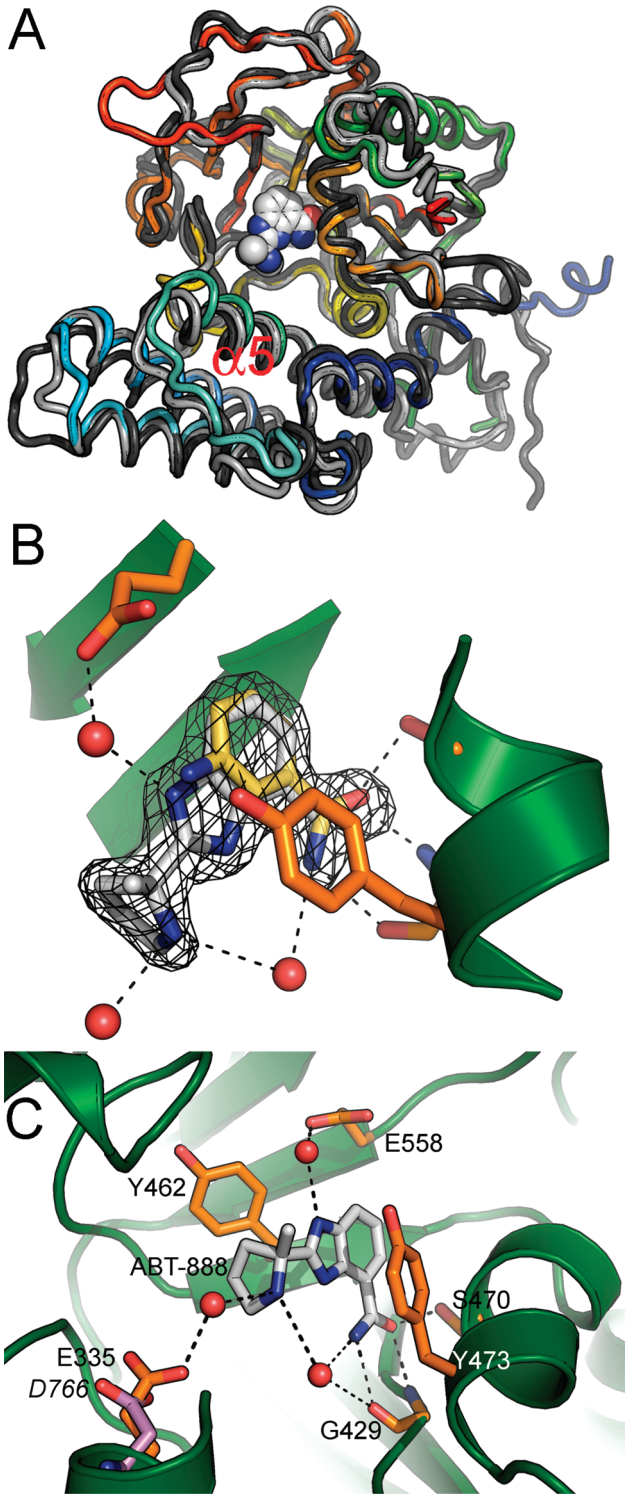

FIGURE 1: (A) Superposition of the catalytic domain structures of the human PARP2-ABT-888 complex (colored), PARP1 (2rd6, light gray), and PARP3 (3c4h, dark gray). The PARP2-bound inhibitor is shown, and α-helix 5 of the N-terminal helix bundle domain is labeled. (B) Superposition of the PARP2 active site with bound 3-AB (yellow) and ABT-888. The σ_A-weighted $F_{obs} - F_{calc}$ electron density map for ABT-888, rendered at 3.5σ, is shown. (C) Detail of the interactions between ABT-888 and PARP2. Selected PARP2 side chains are colored orange, and PARP1 D766 is colored pink.

ACKNOWLEDGMENT

We thank the beamline staff at the DIAMOND synchrotron radiation light source (Oxfordshire, U.K.) for expert assistance during data collection.

SUPPORTING INFORMATION AVAILABLE

Experimental details. This material is available free of charge via the Internet at http://pubs.acs.org.

REFERENCES

1. Amé, J. C., and Spenlehauer, C. (2004) The PARP superfamily. *BioEssays 26*, 882–893.
2. Hassa, P. O., and Hottiger, M. O. (2008) The diverse biological roles of mammalian PARPs, a small but powerful family of poly-ADP-ribose polymerases. *Front. Biosci. 13*, 3046–3082.
3. Amé, J. C., and Rolli, V. (1999) PARP-2, a novel mammalian DNA damage-dependent poly(ADP-ribose) polymerase. *J. Biol. Chem. 274*, 17860–17868.
4. Schreiber, V., and Amé, J. C. (2002) Poly(ADP-ribose) polymerase-2 (PARP-2) is required for efficient base excision DNA repair in association with PARP-1 and XRCC1. *J. Biol. Chem. 277*, 23028–23036.
5. Yélamos, J., and Schreiber, V. (2008) Toward specific functions of poly(ADP-ribose) polymerase-2. *Trends Mol. Med. 14*, 169–178.
6. Augustin, A., and Spenlehauer, C. (2003) PARP-3 localizes preferentially to the daughter centriole and interferes with the G1/S cell cycle progression. *J. Cell Sci. 116*, 1551–1562.
7. Bryant, H. E., and Petermann, E. (2009) PARP is activated at stalled forks to mediate Mre11-dependent replication restart and recombination. *EMBO J. 28*, 2601–2615.
8. Martin, S. A., and Lord, C. J. (2008) DNA repair deficiency as a therapeutic target in cancer. *Curr. Opin. Genet. Dev. 18*, 80–86.
9. Otto, H., and Reche, P. A. (2005) In silico characterization of the family of PARP-like poly(ADP-ribosyl)transferases (pARTs). *BMC Genomics 6*, 139.
10. Thomas, H. D., and Calabrese, C. R. (2007) Preclinical selection of a novel poly(ADP-ribose) polymerase inhibitor for clinical trial. *Mol. Cancer Ther. 6*, 945–956.
11. Plummer, R., and Jones, C. (2008) Phase I study of the poly(ADP-ribose) polymerase inhibitor, AG014699, in combination with Temozolomide in patients with advanced solid tumors. *Clin. Cancer Res. 14*, 7917–7923.
12. Fong, P. C., and Boss, D. S. (2009) Inhibition of poly(ADP-ribose) polymerase in tumors from BRCA mutation carriers. *N. Engl. J. Med. 361*, 123–134.
13. Kummar, S., and Kinders, R. (2009) Phase 0 clinical trial of the poly(ADP-ribose) polymerase inhibitor ABT-888 in patients with advanced malignancies. *J. Clin. Oncol. 27*, 2705–2711.
14. Ruf, A., and Ménnissier de Murcia, J. (1996) Structure of the catalytic fragment of poly(AD-ribose) polymerase from chicken. *Proc. Natl. Acad. Sci. U.S.A. 93*, 7481–7485.
15. Lehtiö, L., and Jemth, A. S. (2009) Structural Basis for Inhibitor Specificity in Human Poly(ADP-ribose) Polymerase-3. *J. Med. Chem. 52*, 3108–3111.
16. Oliver, A. W., and Amé, J. C. (2004) Crystal structure of the catalytic fragment of murine poly(ADP-ribose) polymerase-2. *Nucleic Acids Res. 32*, 456–464.
17. Papeo, G., and Forte, B. (2009) Poly(ADP-ribose) polymerase inhibition in cancer therapy: Are we close to maturity? *Expert Opin. Ther. Pat. 19*, 1377–1400.
18. Penning, T. D., and Zhu, G. D. (2009) Discovery of the poly(ADP-ribose) polymerase (PARP) inhibitor 2-[(*R*)-2-methylpyrrolidin-2-yl]-1H-benzimidazole-4-carboxamide (ABT-888) for the treatment of cancer. *J. Med. Chem. 52*, 514–523.
19. Donawho, C. K., and Luo, Y. (2007) ABT-888, an orally active poly-(ADP-ribose) polymerase inhibitor that potentiates DNA-damaging agents in preclinical tumor models. *Clin. Cancer Res. 13*, 2728–2737.
20. Davis, I. W., and Murray, L. W. (2004) MOLPROBITY: Structure validation and all-atom contact analysis for nucleic acids and their complexes. *Nucleic Acids Res. 32*, W615–W619.